The Role of Solar Heating in the Forcing of the Terdiurnal Tide

F. Lilienthal, Ch. Jacobi

Institute for Meteorology, Stephanstr. 3, 04103 Leipzig,
E-Mail: friederike.lilienthal@uni-leipzig.de

Summary: We use the middle and upper atmosphere model (MUAM) to analyze forcing mechanisms of the terdiurnal tide (TDT) in the middle atmosphere, namely solar heating and nonlinear wave-wave interactions. First, we present model amplitudes of the TDT during January conditions as a validation and for reference. By switching off single forcings for wavenumber 3 in different model runs we are able to separate the solar and nonlinear forcing contribution. The simulations suggest that solar forcing is the major driver for TDT at low latitudes while nonlinear interactions become more important at middle and high latitude, especially in the winter hemisphere. Additionally we observe increased TDT amplitudes for purely solar driven TDTs without nonlinear forcing in some regions which may be owing to destructive interferences.

Zusammenfassung: Wir nutzen das Modell für die mittlere und obere Atmosphäre (MUAM), um die Anregungsmechanismen der dritteltägigen Gezeiten, solare Erwärmung und Wechselwirkungen zwischen Wellen, zu analysieren. Zunächst präsentieren wir die modellierten Amplituden der dritteltägigen Gezeiten für Januarbedingungen. Dies dient einerseits der Validierung und andererseits als Referenz. Indem die Wellenzahl 3 in den verschiedenen Anregungstermen in einzelnen Läufen ausgeschalten wird, lassen sich die jeweiligen Beiträge aus solarer und nichtlinearer Anregung separieren. Aus den Simulationen lässt sich ableiten, dass solare Erwärmung den Hauptanteil in niedrigen Breiten bildet, während nichtlineare Wechselwirkungen in mittleren und hohen Breiten immer wichtiger werden, vor allem auf der Winterhemisphäre. Zudem beobachten wir verstärkte Amplituden der dritteltägigen Gezeiten bei ausschließlich solarer Anregung ohne nichtlinearen Anteil, was an destruktiver Überlagerung der Antriebsterme liegen kann.

1 Introduction

Atmospheric solar tides are one of the most important dynamical features of the mesosphere and lower thermosphere (MLT). They have periods of a solar day and its subharmonics as they are primarily excited by the daily variation of solar heating. They are called „migrating“ when they propagate sun-synchronously and can reach amplitudes that are of the order of the mean wind. Due to the fact that amplitudes are, on an average, smaller for shorter periods, the diurnal tides (DTs) and semidiurnal tides (SDTs) have gained most attraction in the past and are thus better understood than terdiurnal tides (TDTs).

However, TDT amplitudes are comparable with SDT and DT ones on some occasions, e.g. during equinoxes at middle latitudes and may reach amplitudes of 20 m/s or 10 K, respectively. This has been observed using satellites (e.g., Smith, 2000; Pancheva et al., 2013) and radar measurements (e.g., Thayaparan, 1997; Jacobi and Fytterer, 2012). The primary source of atmospheric tides is direct solar heating due to absorption of ultra violet (UV) radiation in the water vapor (troposphere) and ozone (stratosphere) region. However, numerical model studies have shown that this is not sufficient to explain the structure and magnitude of the TDT in the MLT. This was first examined by Glass and Fellous (1975) and later confirmed by, e.g. Teitelbaum et al. (1989); Smith and Ortland (2001); Akmaev (2001); Huang et al. (2007). Further possible excitation mechanisms are nonlinear interactions (Glass and Fellous, 1975; Teitelbaum et al., 1989), gravity wave-tidal interactions and mean flow-tidal interactions (Huang et al., 2007), but their role is still under debate. Teitelbaum et al. (1989) found that nonlinear interactions and direct solar forcing may produce TDTs of comparable amplitudes. Smith and Ortland (2001) performed a model study using a nonlinear model with specified DT and SDT fields at the lower boundary. They were switching off the terdiurnal solar component on the one hand and removing the direct forcing of SDTs on the other hand to eliminate nonlinear interactions between DTs and SDTs. They concluded that solar forcing is dominant at middle and high latitudes while nonlinear interactions mainly contribute at low latitudes. A similar approach was used by Akmaev (2001) and the result was that solar heating from the ozone region is the main source, but noticeable nonlinear in-situ contribution is found during equinoxes. Huang et al. (2007) used a fully nonlinear tidal model with specified diurnal and semidiurnal thermotidal heating so that observed TDT amplitudes were only possible due to nonlinear interactions and they were indeed significant in the MLT. A more recent model study about terdiurnal forcing mechanisms (Du and Ward, 2010) included self-consistent tides due to radiative heating, convective processes and latent heat release. Using a correlation analysis of DT and SDT with TDT on a seasonal and short-term scale they could not identify significant nonlinear interactions and stated that solar heating is the major source of TDTs.
To conclude, the results concerning the relative contributions of different forcing terms of the TDT are still not clarified and partly contradicting. Therefore, in the following model study about the excitation mechanisms of the TDT we use a mechanistic global circulation model with a new approach to separate the solar and nonlinear forcing. Similar to Smith and Ortland (2001) and Akmaev (2001) we remove the wavenumber 3 component of the solar heating in a first simulation. Additionally we perform a simulation where we remove wavenumber 3 from the nonlinear terms, namely the advection terms and the adiabatic heating in the prognostic equations. This procedure is described in more detail in section 2 and the results of these simulations are presented in section 3. In section 4 we give a short conclusion and set the results into context with previous investigations.

2 Model Description and Experimental Setup

We use a mechanistic global circulation model of the middle atmosphere called MUAM. It is a nonlinear primitive equation model with a horizontal resolution of $5 \times 5.625^\circ$ and it extends up to an altitude of 160 km in log-pressure height in steps of 2.842 km. This is described in detail by Pogoreltsev et al. (2007). At the lower boundary of the

model (1000 hPa) zonal means of temperature and geopotential derived from ERA-Interim reanalyses are assimilated and for temperature also up to an altitude of 30 km to correct the climatology in the troposphere and lower stratosphere.
Within the model, solar tides can either be created directly through absorption of solar radiation or nonlinearly as a result of an interaction between other waves. A solar heating parameterization computes heating rates for H_2O, CO_2, O_2, O_3 and N_2 based on Strobel (1978) with further improvements described by Fröhlich et al. (2003). The daily variation of these heating rates creates tides self-consistently. The TDT has been modeled using MUAM by Fytterer et al. (2014), who compared TDT wind shear from the model with global lower ionospheric electron density maxima, and Krug et al. (2015) presented a seasonal climatology of the TDT based on MUAM simulations. Zonal mean ozone fields are taken from the Stratosphere-troposphere Processes And their Role in Climate project (SPARC; Randel and Wu, 2007). The volume mixing ratio for carbon dioxide has been adjusted according to measurements from Mauna Loa Observatory for the year 2005 (378ppm; NOAA ESRL Global Monitoring Division, 2015).
Nonlinear interactions of waves may contribute to tidal forcing. These interactions can take place by the advection of wind and temperature or adiabatic heating within the tendency equations. The advection terms in spherical coordinates (Eqns. 1-3) and the adiabatic heating (Eqn. 4) may be represented as follows:

$$\vec{v} \cdot (\nabla u) = \frac{u}{a\cos\phi}\frac{\partial u}{\partial \lambda} + \frac{v}{a\cos\phi}\frac{\partial (u\cos\phi)}{\partial \phi} + \frac{w}{\rho_0}\frac{\partial}{\partial z}(\rho_0 u), \tag{1}$$

$$\vec{v} \cdot (\nabla v) = \frac{u}{a\cos\phi}\frac{\partial v}{\partial \lambda} + \frac{v}{a\cos\phi}\frac{\partial (v\cos\phi)}{\partial \phi} + \frac{w}{\rho_0}\frac{\partial}{\partial z}(\rho_0 v), \tag{2}$$

$$\vec{v} \cdot (\nabla T) = \frac{u}{a\cos\phi}\frac{\partial T}{\partial \lambda} + \frac{v}{a\cos\phi}\frac{\partial (T\cos\phi)}{\partial \phi} + \frac{w}{\rho_0}\frac{\partial}{\partial z}(\rho_0 T), \tag{3}$$

$$\left.\frac{\partial T}{\partial t}\right|_{adiab} = \frac{RwT}{m' c_p H}\ , \tag{4}$$

where $\vec{v}$ is the wind vector, u and v are the horizontal wind components, w is the vertical wind component and T is the temperature. a is the Earth's radius, ϕ, λ and z are latitude, longitude and altitude, respectively, and ρ_0 is the basic density. R is the gas constant for dry air, m' is the ratio of molecular weights at the respective altitude and at 1000 hPa, c_p is the specific heat at constant pressure and H is the model's scale height given by 7 km.
Separating the variables into their mean and a perturbation we get, as an example:

$$\frac{u}{a\cos\phi}\frac{\partial u}{\partial \lambda} = \frac{(\overline{u}+u')}{a\cos\phi}\frac{\partial(\overline{u}+u')}{\partial \lambda} = \frac{1}{a\cos\phi}\left(\overline{u}\frac{\partial \overline{u}}{\partial \lambda} + \overline{u}\frac{\partial u'}{\partial \lambda} + u'\frac{\partial \overline{u}}{\partial \lambda} + u'\frac{\partial u'}{\partial \lambda}\right). \tag{5}$$

Analogue results can be retrieved for the other terms. The last term of Eqn. 5 represents the interaction between waves which can create further waves with the sum and the difference of the original frequencies, e.g. a TDT from the DT and SDT interaction.
To analyze the forcing mechanisms of the TDT in the MUAM we remove wavenumber 3 longitudinal variation of the total solar heating rates (run A) and the nonlinear advection terms (run B). By applying this method we can analyze the remaining TDT in both runs. Run A will therefore show a TDT which only exists due to nonlinear interactions while run B will show a purely solar forced TDT.

For comparison of the following results, Fig.1 presents the temperature (left) and zonal wind (right) amplitudes of the migrating TDT from a reference run without removing the wavenumber 3 from neither the nonlinear nor the solar terms. The results are representative for January and show strong maxima of more than 10 K and 10 m/s, respectively, above 120 km altitude at low and middle latitudes. At the equator, the tide almost vanishes. Amplitudes are generally decreasing towards the poles but we also find secondary maxima at middle to high latitudes.

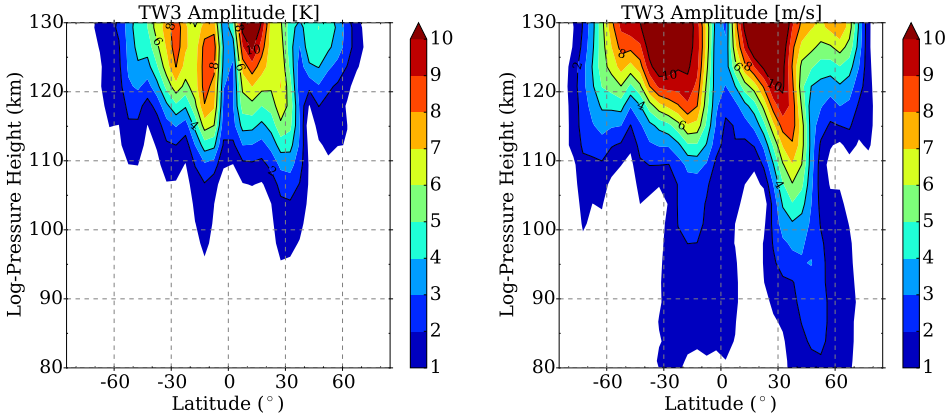

Fig. 1: Amplitudes of the migrating TDT as derived from a reference model run for January conditions. Left panel: Temperature. Right panel: Zonal wind.

3 Model results removing wavenumber 3

As discussed above, the most important forcing mechanisms of TDTs are the absorption of solar radiation and nonlinear interactions between other waves, namely DT and SDT. Fig. 2 shows the migrating terdiurnal components (wavenumber 3 and period of 8 h) of these forcings for different altitudes where the nonlinear forcing is split into its parameters for zonal wind, meridional wind and temperature, according to Eqns. 1-3. On the one hand, it can be clearly seen that solar heating is the dominant feature in the lower atmosphere with a maximum of about 3.5 K/d at 50 km altitude, which corresponds to the region where the ozone concentration is largest. Note also that forcing from the troposphere, in the water vapor absorption band, is not evident which is, however, partly owing to the zonal mean water vapor climatology introduced in MUAM. On the other hand, the nonlinear terdiurnal forcing is continuously increasing with height but very small below 80 km altitude. It reaches its maximum in the mesosphere between 110 and 120 km. The forcing in zonal and meridional wind reaches more than 20 m/s/d each while the temperature wave forcing reaches about 20 K/d. Due to absorption of extreme UV radiation, the terdiurnal solar forcing shows a second maximum around 125 km altitude, but compared to the nonlinear thermal forcing it is still smaller. From these results we can assume that terdiurnal forcing due to solar heating is dominant at lower altitudes while nonlinear interactions mainly contribute in the upper atmosphere.

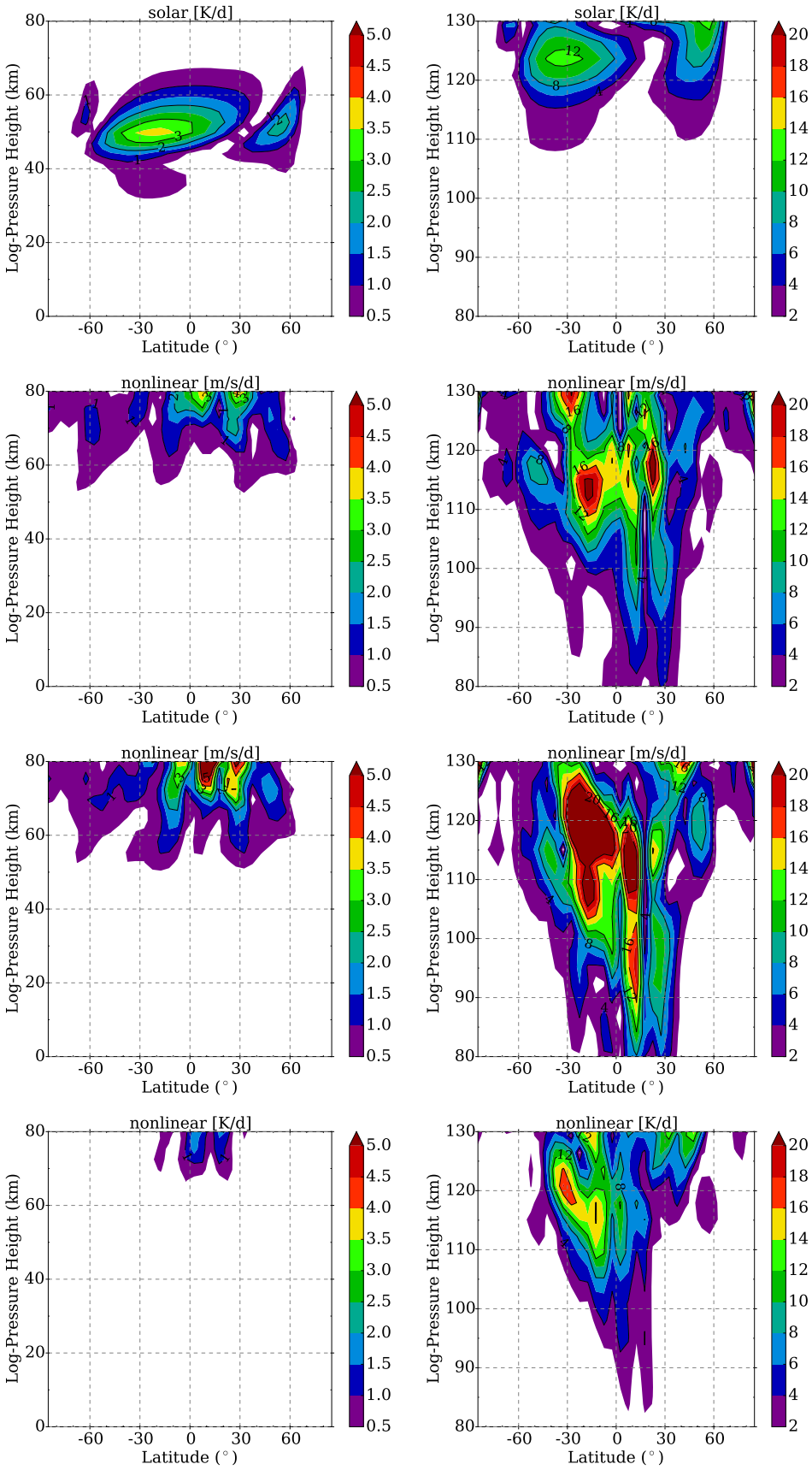

Fig. 2: From top to bottom: Terdiurnal component of the solar forcing (total heating rates), nonlinear zonal forcing (from Eqn. 1), nonlinear meridional forcing (from Eqn. 2) and nonlinear temperature forcing (from Eqn. 3). Left panels: lower atmosphere until 80 *km altitude. Right panels: upper atmosphere from* 80-130 *km altitude.*

To separate the impact of these two forcing mechanisms we perform two different model runs A and B as described in the previous section. The resulting amplitudes for the terdiurnal tide in temperature and zonal wind are shown in Figs. 3 and 4.
Compared with the reference run in Fig. 1, the amplitudes for purely nonlinearly forced terdiurnal tides, i.e. for the tide that is solely originating from nonlinear interaction (run A; Fig. 3) are drastically reduced. The strong maxima of the temperature amplitude at low latitudes disappeares in Fig. 3 (left) and we obtain a small maximum of about 4 K at northern mid-latitudes instead. In this region, however, this represents a relatively large contribution considering that the reference amplitude in this region is only 5 to 6 K. Amplitudes larger than 1 K can only be found above 110 km (120 km) altitude in the northern (southern) hemisphere which is about 10 km higher than in the reference run. The terdiurnal amplitudes in zonal wind (Fig. 3, right) show a 6 m/s maximum at northern high latitudes which is again relatively large compared to the reference with not more than 8 m/s in this region. Secondary maxima of about 2-4 m/s at northern low latitudes and southern high latitudes can be seen as well but these are comparably small. Thus, the TDT is generally much smaller without solar forcing and the strong low latitude TDT cannot be explained by nonlinear interactions. However, nonlinear interactions contribute at most latitudes and at northern (winter) high latitudes the nonlinear forcing seems to be a major driver of TDTs.
The TDT amplitudes for run B, i.e. with nonlinear interactions turned off, and their differences to the reference run are shown in Fig. 4. In other words, the figure represents the results for a purely solar driven TDT. The global structure of TDT amplitudes in the MLT remains similar to the structure in the reference run. Quantitative changes can be obtained from Fig. 4c and d showing that strong changes only appear above 110 km for the temperature amplitudes and above 100 km for the zonal wind amplitudes. Regarding temperature (Fig. 4c), the amplitudes at low latitudes are increased by up to 2 K between 120 – 130 km altitude. At northern mid-latitudes amplitudes are reduced by 1 – 2 K but the differences become almost zero towards the poles where the total amplitude (Fig. 4a) reaches zero as well. For zonal wind amplitudes (Fig. 4d) we obtain an increase of slightly more than 2 m/s at northern low latitudes. Northern mid-latitudes reveal an increase by about 1 m/s at about 110 km altitude. In higher altitudes (above 120 km) at about 70°N amplitudes are decreased by up to 3 m/s. Differences in the southern (summer) hemisphere are generally smaller not exceeding values of ±1 m/s.
The significant positive changes in run B, i.e. at low latitudes, may be explained by destructive interferences between the solar driven wave and the nonlinear forcing. If they act opposite to each other, a removed nonlinear forcing may lead to an increase in amplitude because the solar driven wave can then freely propagate into the upper atmosphere without being suppressed. However, this needs to be further analyzed.

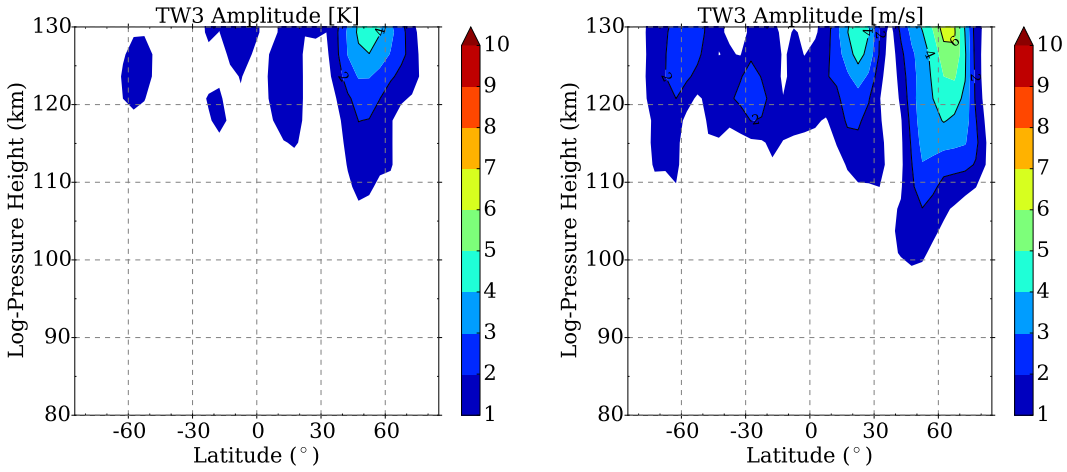

Fig. 3: Amplitudes of TDTs in a latitude-height cross section for temperature (left) and zonal wind (right) corresponding to a model run without wavenumber 3 in solar heating.

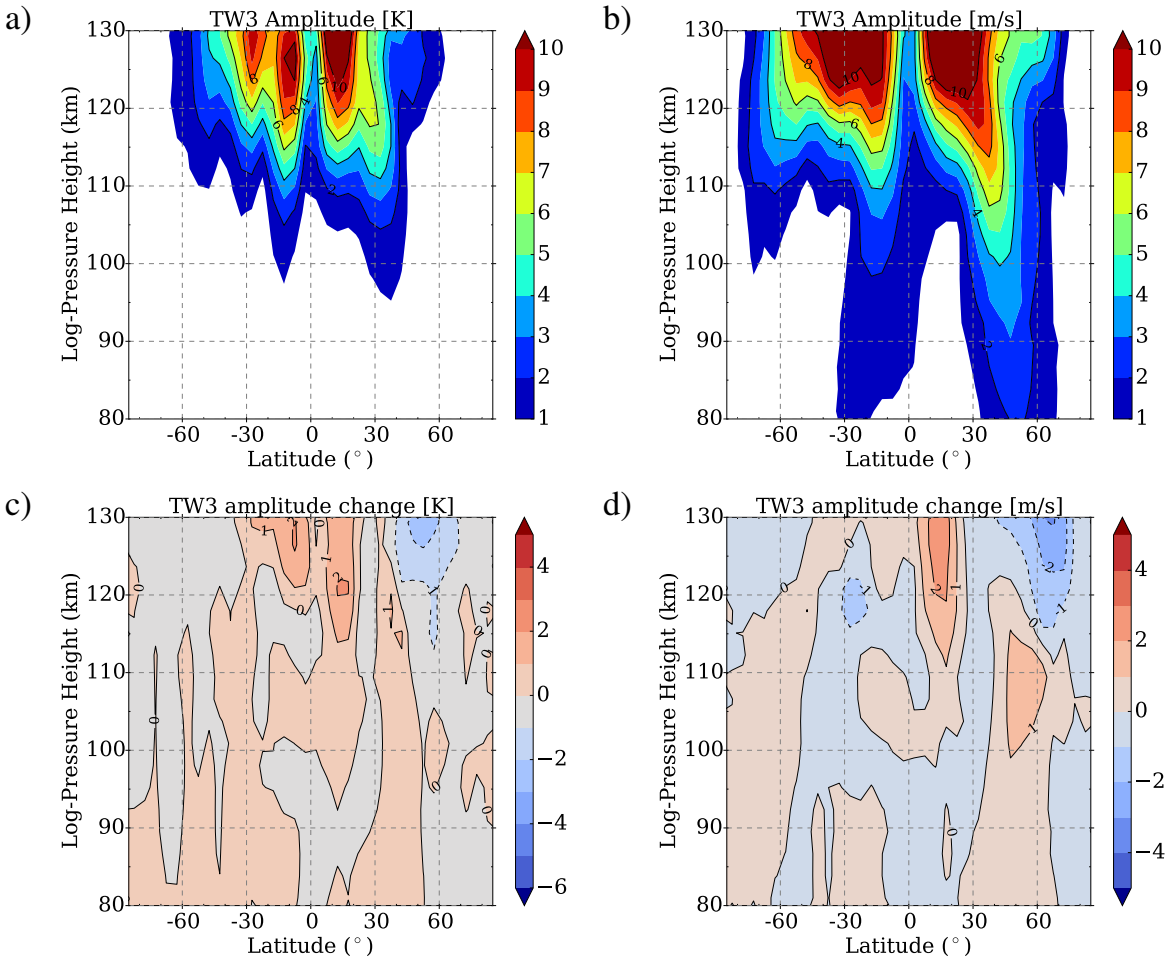

Fig. 4: Amplitudes of TDTs in a latitude-height cross section for temperature (a) and zonal wind (b) corresponding to a model run without wavenumber 3 in all nonlinear advection terms. TDT amplitude differences to the reference for temperature (c) and zonal wind (d). Red (blue) colors indicate larger (smaller) amplitudes in the modified run without wavenumber 3 than in the reference run.

4 Discussion and Conclusion

In order to describe the forcing mechanisms of the TDT in the middle atmosphere we performed numerical simulations using a nonlinear global circulation model. The structure and magnitude of the TDT is in good agreement with observations: for January conditions we get amplitudes up to 10 K in temperature and larger than 10 m/s in zonal wind, respectively. The maxima are located above 120 km altitude at low latitudes. A more detailed climatology and comparison with observations is already published by Krug et al. (2015).

As pointed out by Glass and Fellous (1975), Teitelbaum et al. (1989) and others, the most important forcing mechanisms of the TDT are absorption of solar radiation in the ozone heating region and nonlinear interactions between tides. To separate these forcings in the model, we performed two different runs additionally to the reference run. In run A we removed wavenumber 3 from the solar forcing to analyze pure nonlinearly driven TDT and in run B we removed wavenumber 3 from the nonlinear terms in the tendency equations to get the result of a purely solar driven TDT. In our simulations the solar forcing clearly dominates at low latitudes while a stronger contribution of nonlinear forcing is found at northern (winter) middle and high latitudes. This supports the results of Huang et al. (2007) who also found significant amplitudes due to nonlinear interactions. Akmaev (2001) removed wavenumber 3 from the solar heating, similar to our run A, and showed wind and temperature amplitude profiles for 44°N during winter. For zonal wind he obtained a rather small nonlinear contribution which is in accordance with our results that show a clear gap of zonal wind amplitudes around 40°N. In temperature, the nonlinear forcing becomes significant above 100 km which is also in accordance to our results, but in our simulations, amplitudes start to be significant only above 110 km. Our results do not support those of Du and Ward (2010) who found that solar forcing is the only important mechanism but they used correlation analyses between DT and TDT instead of removing certain forcings. Smith and Ortland (2001) performed similar model runs like our run A and B. They found that nonlinear interactions at 97 km altitude are more important at low latitudes but during January the amplitudes of TDTs without solar forcing are small everywhere in their simulations and are thus difficult to interpret. For the run without nonlinear forcing they found large amplitudes at 97 km at middle and high latitudes in the zonal wind component. In these altitudes, our model results are similar showing a maximum around 50°N.

Furthermore, we observe that TDT amplitudes are regionally increased when the nonlinear forcing is switched off. To our knowledge, this has not been reported before. However, earlier model studies (e.g., Smith and Ortland, 2001) removed the nonlinear forcing by switching off the solar SDT to avoid interactions between DT and SDT. Here, we use a new and possibly more accurate approach modifiing the nonlinear terms within the prognostic equations. A possible explanation for these increased amplitudes are destructive interferences between the solar driven TDT and the nonlinear forcing. Further analyses about this topic are necessary and will be considered in the future.

Acknowledgements

ECMWF reanalyses data are provided by apps.ecmwf.int/datasets/data/ and have been used in MUAM for assimilation in the troposphere. The study has been supported by Deutsche Forschungsgemeinschaft under grant JA 836/30-1.

References

Akmaev, R., 2001: Seasonal variations of the terdiurnal tide in the mesosphere and lower thermosphere: a model study, Geophys. Res. Let., 28, 3817–3820.

Du, J. and Ward, W., 2010: Terdiurnal tide in the extended Canadian Middle Atmospheric Model (CMAM) , J. Geophys. Res., 115, D24 106, doi:10.1029/2010JD014479.

Fröhlich, K., Pogoreltsev, A., and Jacobi, C., 2003: The 48 Layer COMMA-LIM Model: Model description, new Aspects, and Climatology, Rep. Inst. Meteorol. Univ. Leipzig, pp. 161–189, URL: www.uni-leipzig.de/%7Ejacobi/medec/2003_COMMA_LIM.pdf.

Fytterer, T., Arras, C., Hoffmann, P., and Jacobi, C., 2014: Global distribution of the migrating terdiurnal tide seen in sporadic E occurrence frequencies obtained from GPS radio occultations, Earth Planets Space, 66, 1–9, doi:10.1186/1880-5981-66-79.

Glass, M. and Fellous, J. L., 1975: The eight-hour (terdiurnal) component of atmospheric tides, Space Res., 15, 191–197.

Huang, C., Zhang, S., and Yi, F., 2007: A numerical study on amplitude characteristics of the terdiurnal tide excited by nonlinear interaction between the diurnal and semidiurnal tides, Earth Planets Space, 59, 183–191.

Jacobi, C. and Fytterer, T., 2012: The 8-h tide in the mesosphere and lower thermosphere over Collm (51.3°N; 13.0°E), 2004–2011, Adv. Rad. Sci., 10, 265–270, doi:10.5194/ars-10-265-2012.

Krug, A., Lilienthal, F., and Jacobi, C., 2015: The terdiurnal tide in the MUAM circulation model, Rep. Inst. Meteorol. Univ. Leipzig, 53, 33–44, uni-leipzig.de/ meteo/de/orga/LIM_Bd_53.pdf.

NOAA ESRL Global Monitoring Division, 2015: Atmospheric Carbon Dioxide Dry Air Mole Fractions from quasi-continuous measurements at Mauna Loa, Hawaii, National Oceanic and Atmospheric Administration (NOAA), Earth System Research Laboratory (ESRL), Global Monitoring Division (GMD): Boulder, Colorado, USA, Compiled by K.W. Thoning, D.R. Kitzis, and A. Crotwell, Version 2015-12, updated annually.

Pancheva, D., Mukhtarov, P., and Smith, A., 2013: Climatology of the migrating terdiurnal tide (TW3) in SABER/ TIMED temperatures , J. Geophys. Res.: Space Phys., 118, 1755–1767, doi:10.1002/jgra.50207.

Pogoreltsev, A. I., Vlasov, A. A., Fröhlich, K., and Jacobi, C., 2007: Planetary waves in coupling the lower and upper atmosphere, J. Atmos. Sol.-Terr. Phys., 69, 2083–2101, doi: 10.1016/j.jastp.2007.05.014.

Randel, W. J. and Wu, F., 2007: A stratospheric ozone profile data set for 1979–2005: Variability, trends, and comparisons with column ozone data, J. Geophys. Res.: Atmos., 112, n/a–n/a, doi:10.1029/2006JD007339, D06313.

Smith, A. and Ortland, D., 2001: Modeling and Analysis of the Structure and Generation of the Terdiurnal Tide, J. Atmos. Sci., 58, 3116–3134.

Smith, A. K., 2000: Structure of the terdiurnal tide at 95 km, Geophys. Res, Let., 27, 177–180, doi:10.1029/1999GL010843.

Strobel, D. F., 1978: Parameterization of the atmospheric heating rate from 15 to 120 km due to O2 and O3 absorption of solar radiation, J. Geophys. Res.: Oceans, 83, 6225–6230, doi:10.1029/JC083iC12p06225.

Teitelbaum, H., Vial, F., Manson, A., Giraldez, R., and Massebeuf, M., 1989: International Middle Atmosphere Program Symposium Non-linear interaction between the diurnal and semidiurnal tides: terdiurnal and diurnal secondary waves, J. Atmos. Terr. Phys., 51, 627–634, doi:10.1016/0021-9169(89)90061-5.

Thayaparan, T., 1997: The terdiurnal tide in the mesosphere and lower thermosphere over London, Canada (43°N, 81°W), J. Geophys. Res.: Atmos., 102, 21 695–21 708, doi:10.1029/97JD01839.